Developmental basis of limblessness and axial patterning in snakes

Martin J .Cohn*† & Cheryll Tickle†‡

** Division of Zoology, School of Animal and Microbial Sciences, University of Reading, Whiteknights, Reading RG6 6AJ, UK*
‡ Department of Anatomy and Physiology, Wellcome Trust Building, University of Dundee, MSI/WTB Complex, Dow Street, Dundee DD1 5EH, UK
† Department of Anatomy and Developmental Biology, University College London, Medawar Building, Gower Street, London WC1E 6BT, UK

The evolution of snakes involved major changes in vertebrate body plan organization, but the developmental basis of those changes is unknown. The python axial skeleton consists of hundreds of similar vertebrae, forelimbs are absent and hindlimbs are severely reduced. Combined limb loss and trunk elongation is found in many vertebrate taxa[1], suggesting that these changes may be linked by a common developmental mechanism. Here we show that Hox gene expression domains are expanded along the body axis in python embryos, and that this can account for both the absence of forelimbs and the expansion of thoracic identity in the axial skeleton. Hindlimb buds are initiated, but apical-ridge and polarizing-region signalling pathways that are normally required for limb development are not activated. Leg bud outgrowth and signalling by Sonic hedgehog in pythons can be rescued by application of fibroblast growth factor or by recombination with chick apical ridge. The failure to activate these signalling pathways during normal python development may also stem from changes in Hox gene expression that occurred early in snake evolution.

Limblessness has evolved many times in vertebrate evolution, and is often accompanied by elongation and loss of regional differentiation in the axial skeleton[1]. Snakes evolved from tetrapod lizards and are closely related to mosasaurs, which are Cretaceous marine lizards that had complete forelimbs and hindlimbs and a clearly regionalized axial skeleton[1,2]. Pythons have over 300 vertebrae (Fig. 1a), with ribs on every vertebra anterior to the hindlimbs, except for the atlas (Fig. 1a, b, e). The anterior vertebrae have both ribs (a thoracic feature) and ventral hypopophyses (generally a cervical feature) (Fig. 1b), suggesting that information encoding thoracic identity may have extended into the cervical region and partially transformed these segments. Thus, the entire trunk resembles an elongated thorax (Fig. 1a). There is no morphological evidence of forelimb development. Functional rudimentary hind-

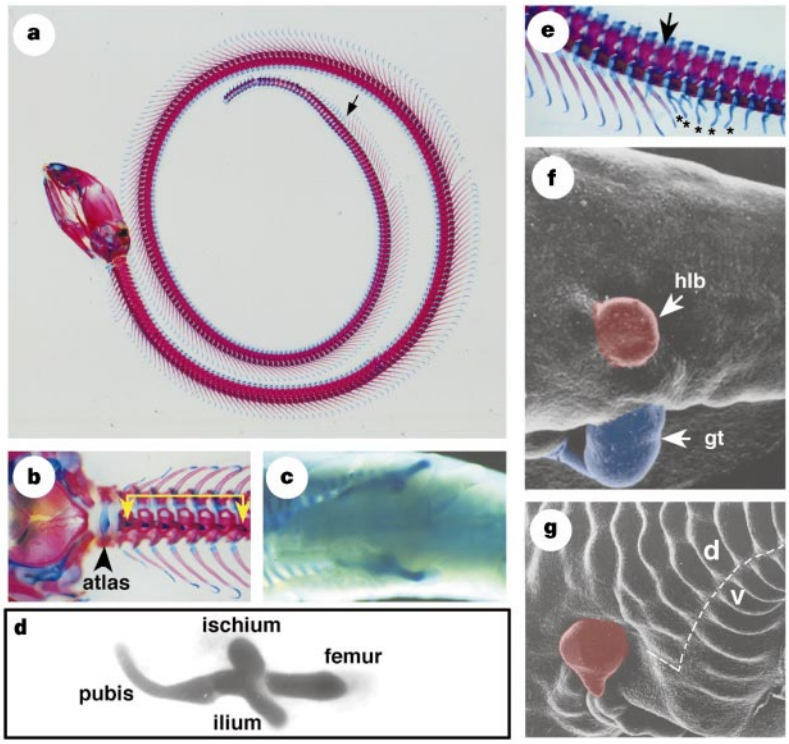

Figure 1 Morphology of python axial and appendicular skeleton. Anterior is to the left. **a**, **b**, **e**, Alcian blue and Alizarin red stained skeletal preparation of python embryo at 24 days of incubation. Arrows mark position of hindlimb rudiments, which have been removed to improve visibility of vertebrae. **a**, Lateral view of complete skeleton. Note homogeneity of vertebrae anterior to arrow. **b**, High-power ventral view of anterior axial skeleton and base of skull. Atlas lacks ribs (arrowhead) and hypopophyses (bracketed), which extend ventrally from 64 vertebral bodies posterior to atlas. **c**, Ventral view of python embryo at 14 days of incubation stained with Alcian green to reveal skeletal pattern. The pelvis is visible within the body wall and short femora protrude from the body wall. **d**, Skeletal preparation of hindlimb and associated pelvis dissected from embryo shown in **c**. Femur and all three elements of pelvic girdle are present (pubis, ilium and ischium). **e**, Skeletal preparation showing cloacal region of python embryo at 24 days of incubation. Arrow indicates position of the hindlimb (removed) relative to axial skeleton. Hindlimb position corresponds to a transitional vertebra with intermediate morphology (arrow), separating vertebrae with large, movable ribs (left) from vertebrae with lymphapophyses in cloacal region (right, with asterisks). **f**, Scanning electron micrograph of left limb bud and trunk of python embryo at 4 days of incubation. Hindlimb bud (hlb; red) lies dorsal to the paired genital tubercles (gt; blue) which develop on the left and right margins of the cloaca. **g**, Scanning electron micrograph of python embryo at 24 days of incubation showing left hindlimb (red); interface between morphologically distinct dorsal scales (d) and ventral belly scales (v), marked by dashed line.

limbs, consisting of a pelvic girdle and truncated femur (Fig. 1c, d), develop at the junction between rib-bearing vertebrae and lymphapophysis-bearing vertebrae, at cloacal level (Fig. 1e, f).

Hox genes specify the axial pattern during embryonic development. In animals with different numbers of vertebrae, Hox expression domains in the paraxial mesoderm (which gives rise to vertebrae) correlate with vertebral identity rather than number[3,4]. Hox genes also appear to be involved in the regionalization of the lateral plate mesoderm into forelimb, flank and hindlimb, to specify limb position[5,6]. To determine whether changes in Hox gene expression in the paraxial and lateral plate mesoderm underlie the morphological transformations seen in the python trunk, we examined the distribution of three Hox proteins, HOXC6, HOXC8 and HOXB5. HOXC6 and HOXC8 are associated with the development of thoracic vertebrae in other tetrapods[7,8] (Fig. 2a), whereas HOXB5 is expressed up to the first cervical vertebra (the atlas)[6,9]. In the lateral plate mesoderm of tetrapods and fish, the anterior expression boundaries of all three genes occur at the forelimb/pectoral fin level, where they are involved in specifying forelimb position and shoulder development[6,10,11]. Python eggs are laid about eight weeks after fertilization, by which time the embryos have developed somites (derived from paraxial mesoderm) and hindlimb buds. In these embryos, HOXC6, HOXC8 and HOXB5 are expressed in somites throughout the entire trunk, extending from the cloacal/hindlimb level to the most anterior somite (Fig. 2b–g). We detected a sharp posterior boundary of HOXC8 expression at the level of the hindlimbs (Fig. 2b), which coincides with the last thoracic vertebra in older animals (compare Fig. 2b with Fig. 1a and e). HOXC8 and HOXB5 are present throughout the python lateral plate mesoderm, with expression terminating at the very anterior limit of the trunk (Fig. 2c, f). Thus, the entire vertebral column anterior to the cloaca exhibits patterns of Hox gene expression consistent with thoracic identity, and we were unable to detect restricted Hox expression patterns in the lateral plate mesoderm associated with forelimb position in other tetrapods (Fig. 2h). Expansion of these Hox gene expression domains in both paraxial and lateral plate mesoderm may be the mechanism which transformed the entire snake trunk towards a thoracic/flank identity and led directly to the absence of forelimb development during snake evolution.

The specification of hindlimb position and initiation of budding appears to be normal in python embryos. The outgrowth of vertebrate limb buds depends on the apical ectodermal ridge, a thickened epithelium rimming the distal edge of the limb buds (Fig. 3b)[12]. Although direct-developing frogs undergo normal limb development without forming a distinctive apical ridge, the distal limb bud ectoderm nevertheless expresses genes associated with ridge function[13]. In python embryos between 1 and 5 days of incubation, no apical ridge could be detected either in histological sections or by scanning electron microscopy (Fig. 3a), and products of the *Distal-less* (*Dlx*), *Fgf2* and *Msx* genes, which normally characterize the apical ridge[14–16], were not detected in limb ectoderm (Fig. 3c–h). High levels of expression of these genes were detected in python limb mesenchyme and/or other developing organs (for example, kidneys, tooth buds and scale buds), demonstrating that the antibodies we used can recognize the reptilian gene products. The absence of apical ectodermal ridge and lack of

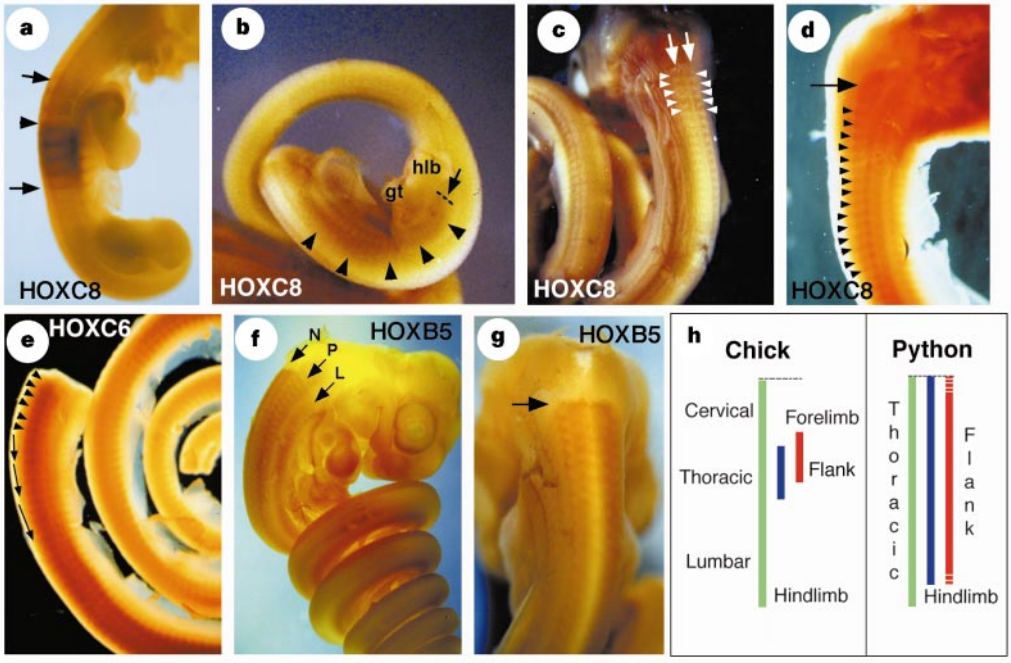

Figure 2 Whole-mount antibody staining showing Hox gene expression in python and chick embryos. Anterior is at the top in **a** and **c–h**, and at bottom in **b**. Positive signal is indicated by darkly stained cells. **a**, HOXC8 expression is restricted to thoracic region in chick embryo at stage 25. Arrow, anterior and posterior boundaries; arrowhead, boundary between strong and weak expression. **b–d**, Expression of HOXC8 throughout the trunk of python embryos at one day incubation. **b**, HOXC8 expression (arrowheads) extends posteriorly to level of hindlimb bud (hlb). Dashed line marks the sharp posterior expression boundary. **c**, **d**, Anterior HOXC8 expression in cleared (**d**) and uncleared (**c**) python embryos. Segmental pattern of expression (arrowheads) is detected in prevertebrae up to the anterior limit of the axial skeleton (arrows). **e**, HOXC6 expression in a python embryo. Segmental expression (arrowheads) is detected throughout the entire trunk posterior to the head, which has been removed, in a pattern similar to HOXC8. **f**, **g**, HOXB5 expression detected throughout trunk of python embryo, with sharp anterior boundary of expression in neural tube at the junction of the spinal cord and hindbrain (arrow in **g**). **f**, Anterior boundaries of expression domains (arrows) in neural tube (N), paraxial (P) and lateral plate (L) mesoderm are in register with one another. **h**, Schematic diagram comparing expression domains of HOXB5 (green), HOXC8 (blue) and HOXC6 (red) in chick and python embryos. Broken line at anterior and posterior extremes of red line indicates lack of certainty about precise limits of HOXC6 expression. Expansion of HOXC8 and HOXC6 domains in python correlates with expansion of thoracic identity in axial skeleton and flank identity in lateral plate mesoderm.

expression of ridge-associated genes could account for the severe hindlimb truncation seen in pythons.

Apical ectodermal ridge signalling is mediated by fibroblast growth factors (FGFs)[17,18]. Therefore, we tested whether grafting FGF2-loaded beads to python limb bud could sustain outgrowth. The proximodistal length of FGF2-treated limb buds was increased compared with the contralateral buds in two out of five embryos treated. One day after grafting, a 31% increase was seen with one FGF bead and a 9% increase was seen with two FGF beads. Thus, python limb bud outgrowth can be stimulated by FGF. As FGF can also promote proliferation in cultured vestigial limb buds of the slow-worm *Anguis fragilis*[19], a serpentiform lizard, our results raise the possibility that the independent evolution of limblessness in different reptilian lineages may have involved similar developmental mechanisms.

In amniote limbs, the apical ridge forms at the boundary of the dorsal and ventral ectodermal compartments[20]. A dorsoventral interface between the morphologically distinct dorsal and ventral scales can be seen extending along the entire trunk ectoderm of python embryos, and the paired hindlimb buds develop at this interface (Fig. 1g). The failure of ridge development in chicken *limbless* mutants is due to a lack of dorsoventral polarity in the limb buds[21]. Therefore, we examined python limb buds for expression of two molecules associated with dorsoventral polarity, Engrailed (EN) and LMX1. Just as in normal chick limb buds[22] (Fig. 4i), EN was detected in the ventral ectoderm of python limb buds, with a sharp boundary of expression running along the bud apex (Fig. 4h). In addition, LMX1 (ref. 23) was confined to dorsal limb mesenchyme cells in pythons (Fig. 4j). Thus, python leg buds, in contrast to the limb buds of chicken *limbless* mutants, have normal dorsoventral polarity.

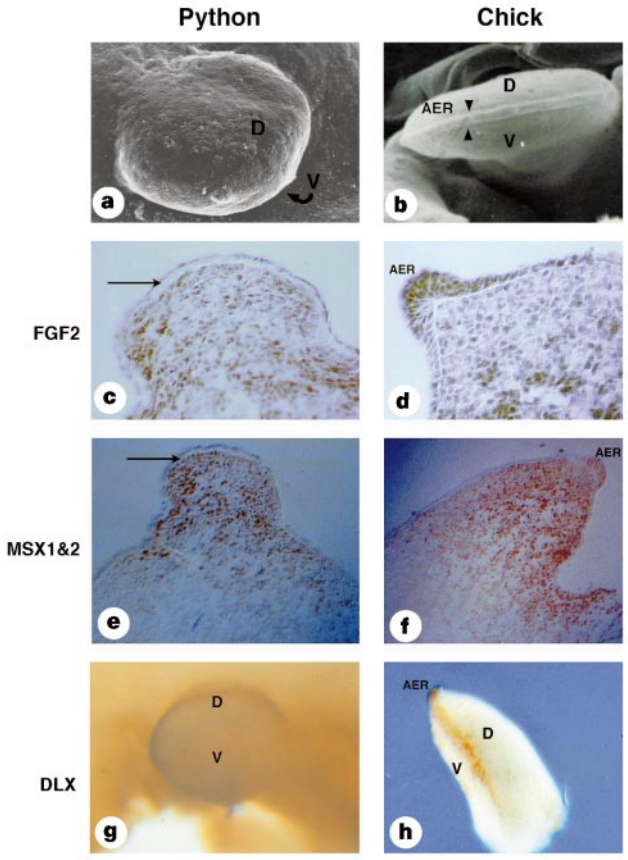

Figure 3 Antibody staining and scanning electron micrographs comparing apical ectoderm in python and chick limb buds. **a**, **b**, Scanning electron micrographs of a python embryo limb bud at 4 days (**a**) and chick embryo at 5 days of incubation (**b**). Distal tip of python bud lacks epical ectodermal ridge (**a**), in contrast to chick, which has a distinct ridge (AER) at the boundary between dorsal (D) and ventral (V) ectoderm (**b**). Transverse sections of python limb buds at 1 day of incubation (**c**, **e**, **g**) and stage 20 chick leg buds (**d**, **f**, **h**) stained with antibodies against FGF2, MSX, and DLX. **c**, FGF2 expression is present in python limb bud mesenchyme but could not be detected in the ectoderm (arrow). **d**, FGF2 expression is present in chick limb bud mesenchyme and ectoderm, with strong expression in apical ectodermal ridge. **e**, MSX expression is present in python limb bud mesenchyme in a proximal-to-distal gradient, but not in ectoderm (arrow). **f**, MSX expression is present in chick limb bud mesenchyme in a proximal-to-distal gradient, and in the apical ectodermal ridge (AER). **g**, DLX expression could not be detected in the python limb. **h**, DLX expression in the apical ectodermal ridge (AER) of chick leg bud.

Another possible reason for the failure of ridge formation is that mesenchymal changes have occurred in python hindlimb buds. To test the ability of python limb bud mesenchyme to signal to the ectoderm, we transplanted mesenchyme from the posterior of the python limb bud to the anterior chick wing bud, and then monitored expression of chick *Fgf8* to determine the extent of the apical ridge. At 19.5 h after transplantation, *Fgf8* expression was detected in anterior chick limb ectoderm overlying the python graft, whereas expression in the contralateral limb did not extend as far to the anterior (Fig. 4g). Thus, python limb mesenchyme can maintain an apical ectodermal ridge and *Fgf8* expression.

Mesenchymal cells in the polarizing region, located at the posterior margin of vertebrate limb buds, act as a signalling centre and express Sonic hedgehog (SHH), which specifies the anteroposterior pattern of the limb. The polarizing region and apical ridge maintain each another through a positive feedback loop, mediated by SHH and FGF4, which coordinates limb bud outgrowth and patterning[17,18]. When *Shh* is functionally inactivated in mice, their limbs are truncated[24]. We therefore examined *Shh* expression in python embryos, which lack an apical ridge. SHH protein is closely associated with *Shh* messenger RNA in the polarizing region in chick and mouse limb buds (Fig. 4b)[25]. In contrast, no SHH protein could be detected in python hindlimb buds (Fig. 4a). SHH was present, however, in floor plate of the neural tube and in the notochord, both of which are known sites of *Shh* expression in other vertebrate embryos[25]. Thus, in the absence of an apical ridge, *Shh* is not expressed in python hindlimb buds.

Three different assays, however, showed that python hindlimb bud mesenchyme retains remarkable potential to express SHH and act as a polarizing region. In python posterior mesenchyme cells grafted under the apical ridge of a chick wing bud at stage 20, SHH was expressed within 24 h (Fig. 4e). In a second chick wing bud, expression of the SHH receptor *patched*, which is induced in response to SHH signalling[26], was detected in chick limb cells around a python graft 19.5 h after transplantation (Fig. 4f). Finally, a wing bud with a python graft left to develop for seven days contained two additional digits (anterior-to-posterior digit pattern *2-2-2-3-4*), compared with the normal pattern (*2-3-4*) (Fig. 4c). This digit pattern can also be produced by anterior grafts of small numbers of *Shh*-expressing cells[27]. These data show that python hindlimb mesenchyme is competent to express SHH and send a polarizing signal, and suggest that it fails to do so during python hindlimb development because the apical ridge is absent.

Unexpectedly, anterior mesenchyme grafted from python hindlimb also has polarizing potential and induced the development of an additional digit 2 in a chick wing (Fig. 4d). Thus, polarizing potential appears to exist both anteriorly and posteriorly in python hindlimb buds, rather than being posteriorly restricted as in other vertebrates. Moreover, three grafts of python lateral plate mesenchyme anterior to the hindlimb bud suggested that polarizing potential is also present in the flank. Several lines of evidence indicate that Hox gene-expression domains along the primary body axis define the spatial extent of polarizing potential. For

example, anterior extension of the *Hoxb8* domain in transgenic mice induces *Shh* expression anteriorly in the forelimb[28]. Thus, widespread polarizing potential in pythons is consistent with our finding that Hox expression domains are expanded anteroposteriorly. Furthermore, since positional information in the limb ectoderm is determined initially by the underlying mesoderm[29], it is possible that changes in mesodermal Hox gene expression in pythons may also have eliminated the ability of the ectoderm to form an apical ridge.

A simple developmental mechanism involving progressive changes in Hox gene expression along the main body axis could link expansion of thoracic identity with acquisition of limblessness in snake evolution (Fig. 5). The primitive condition for all squamates, including snakes, is possession of complete forelimbs and hindlimbs, and a relatively short, regionalized vertebral column. The most primitive snake known, *Pachyrhachis problematicus*, had complete (or almost complete) polarized hindlimbs, but no forelimbs, and an elongated vertebral column with ribs on almost every segment[2]. Both scolecophidians and booids (which includes pythons) are primitive snakes with severely reduced hindlimbs and a trunk resembling an elongated thorax. Advanced snakes (colubroids) have even more uniformity in the axial skeleton and are completely limbless. Progressive expansion of Hox gene expression domains along the body axis can account for the major

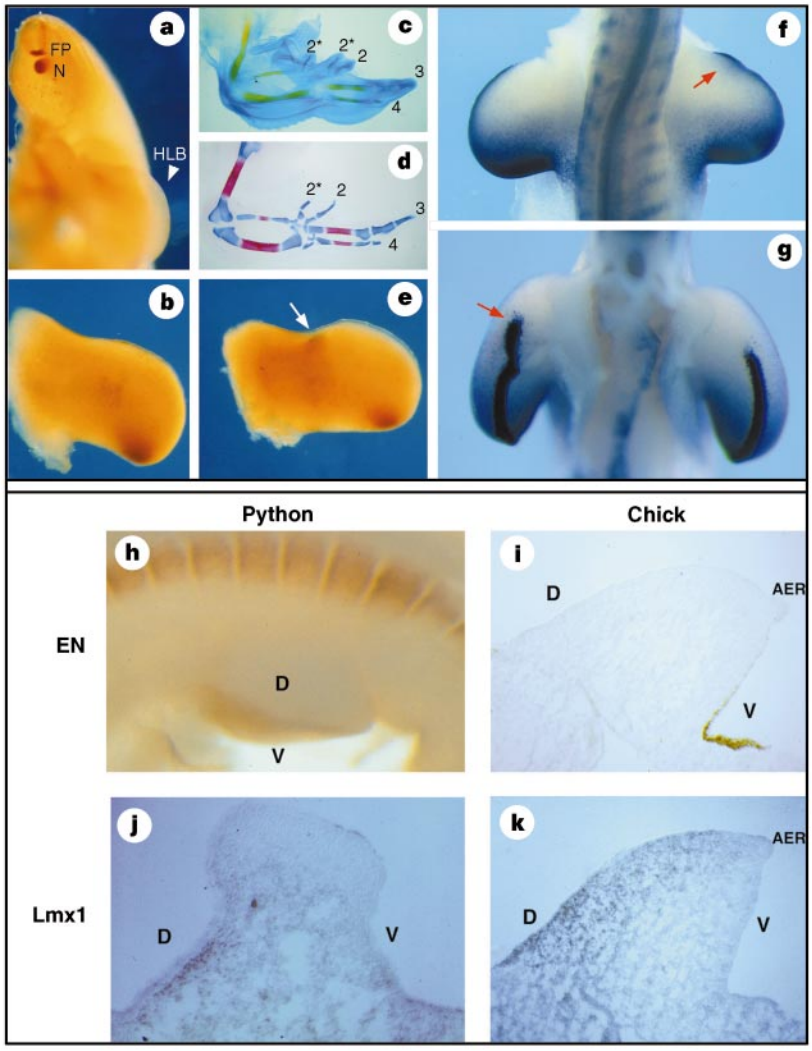

Figure 4 Polarizing activity and dorsoventral polarity in python hindlimb buds. Anterior is at top in **a–g** and at right in **h**. **a**, Python embryo at 2 days of incubation stained with an antibody against SHH. SHH expression (dark brown) detected in floor plate (FP) and notochord (N), but not in hindlimb bud (HLB). **b**, SHH expression in polarizing region of chick wing bud. **c**, Wing of ten-day chick embryo with duplicated pattern of digits that developed after transplantation of python posterior limb bud mesenchyme to anterior margin of wing bud at stage 20. Two additional digit 2s were specified anterior to the normal set of digits. (asterisk, duplicated digits). **d**, Wing of ten-day chick embryo with duplicated pattern of digits that developed after transplantation of python anterior limb bud mesenchyme to anterior margin of wing bud at stage 20. A single duplicated digit 2 is present anterior to normal digits. **e**, SHH expression in chick wing bud 24 h after python posterior limb mesenchume was grafted anteriorly under the apical ridge. SHH expression was detected in the graft of python cells (arrow) and in the host chick polarizing region. **f**, **g**, Double *in situ* hybridization showing expression of chick *Ptc* and *Fgf8* 24 h after transplantation of python posterior limb mesenchyme to anterior margin of the chick right wing bud. Red arrow in **f** (dorsal view) indicates ectopic expression of chick *Ptc* in anterior mesenchyme around grafted python cells. Red arrow in **g** (ventral view) indicates anteriorly extended domain of *Fgf8* in chick ectoderm overlying the python mesenchyme cells (compare anterior limit of *Fgf8* expression in limb containing graft (left) with contralateral limb (right). **h–k**, Dorsoventral polarity in python limb buds. Antibody staining of EN and LMX1 in python limb buds at 1 day of incubation and chick limb buds at stage 20. **h**, **i**, Expression of EN is detected in ventral ectoderm of python (**h**) and chick (**i**) limb buds. EN expression is also seen in python somites (**h**). Expression of LMX1 is detected in dorsal mesenchyme of python (**j**) and chick (**k**) limb buds. D, dorsal; V, ventral.

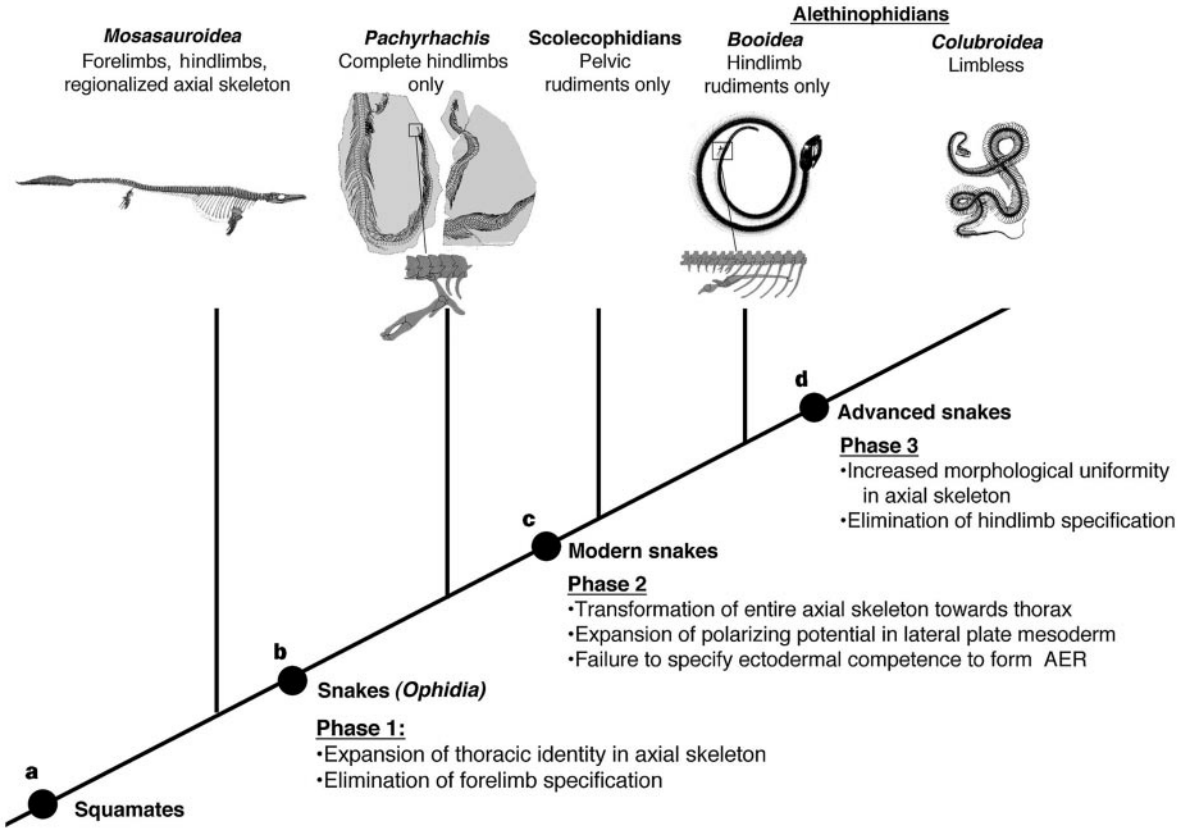

Figure 5 Developmental model for the evolution of snakes. The tree shows the evolutionary relationships among the following: *Colubroidea* (advanced snakes) which lack both forelimbs and hindlimbs and have a large number of nearly-identical vertebrae; *Booidea* (including pythons and boas) which lack forelimbs, but have rudimentary hindlimbs and a large number of morphologically uniform vertebrae with few or equivocal regional differences; Scolecophidians, which have pelvic rudiments and a large number of morphologically uniform vertebrae; the primitive snake *Pachyrhachis problematicus*, which lacks forelimbs, but has complete (or nearly complete) hindlimbs and a large number of similar vertebrae which nonetheless have identifiable regional differences; and mosasaurs, which have a short, morphologically regionalized axial skeleton and complete, normally polarized forelimbs and hindlimbs. According to this model, progressive expansion of Hox gene expression domains can account for loss of forelimbs, hindlimbs and regional identity in the axial skeleton. Additionally, the increase in vertebral number probably required continuous production of mesoderm for axial elongation, and this could have been achieved by sustained growth of the tail bud and movement of mesoderm through the primitive streak[30]. Node **a** indicates the origin of squamates. **b**, Hox expansion initiated before the divergence of the *Pachyrhachis* lineage could have led to the reduction of regional differentiation in the axial skeleton and elimination of forelimb specification, with hindlimb development remaining unaffected. **c**, Continued expansion of Hox domains after the divergence of the *Pachyrhachis* lineage could have led to transformation of the entire axial skeleton (anterior to the tail) towards thoracic identity and to reduction of hindlimb development by eliminating ectodermal competence to form an apical ridge and expanding polarizing potential (competence to express *Shh*). This condition is retained in scolecophidians and in modern pythons, which together with boas comprise the *Booidea*. **d**, Further homogenization of Hox gene expression domains is predicted to have led to the origin of advanced snakes/*colubroidea*. (Phylogenetic relationships among these taxa based on ref. 2; figures are modified from refs 32, 33.)

morphological transitions in snake evolution (Fig. 5). Such higher-order genetic changes could have resulted in sudden anatomical transformations, rather than gradual changes, during snake evolution, a hypothesis which can be tested by the fossil record. Our model predicts that embryos of colubroid snakes should show even more homogenization of Hox gene expression domains along the head-to-tail axis than pythons. □

Methods

Whole-mount skeletal preparations. Python embryos to be double-stained for cartilage and bone were fixed in 80% ethanol, then skinned, eviscerated and dehydrated in 96% ethanol. We then incubated them in acetone, rinsed them in 96% ethanol and stained them for 2–6 h in Alcian blue and Alizarin red in 70% ethanol with 5% acetic acid. Embryos were then rinsed in 96% ethanol followed by tap water before clearing in 1% KOH and a graded glycerol series. Embryos stained for cartilage alone were fixed in 5% trichloroacetic acid and stained with Alcian green, then dehydrated in ethanol and cleared in graded glycerol.

Scanning electron microscopy. Embryos were fixed in modified Tyrode's (1% glutaraldehyde) at 4 °C. After post-fixation in 1% osmium in 0.1M phosphate buffer, specimens were dehydrated in graded ethanol, placed in amyl acetate, critical point dried, sputter-coated with gold particles and viewed on a Hitachi S-530 scanning electron microscope.

Whole-mount *in situ* hybridization and immunohistochemistry. Whole-mount *in situ* hybridization was done as described[5] with digoxigenin-labelled riboprobes for chick *Fgf8* and *patched*. Whole-mount antibody staining was performed as described for HOXC6[7], DLX[31], EN[22], SHH[25], HOXB5[23] and HOXC8[23]. These antibodies were raised against *Xenopus* (HOXC6), butterfly (DLX) and mouse (EN, SHH, HOXB5) proteins, and have been shown to recognize the target epitope in a wide range of vertebrates. For immunohistochemistry on frozen sections, embryos were fixed in 4% paraformaldehyde, equilibrated in 30% sucrose, embedded in Tissue-Tek O.C.T. compound and frozen at −80 °C. Serial sections were cut at 10 μm and stained using a Vectastain ABC kit according to manufacturer's instructions.

Tissue transplantation and application of FGF2 beads. Python embryos were washed in PBS buffer, then dissected in culture medium. We removed fragments of mesenchyme from specific locations using electrolytically sharpened tungsten needles and fine forceps. Tissue was incubated in 2% trypsin and ectoderm was removed. (All previous steps were carried out on ice.)

We prepared host chick wing buds by lifting the apical ridge away from the anterior mesenchyme to make a loop. Python tissue was transplanted inside the loop and the chick embryos were then reincubated at 38 °C. FGF beads were prepared as described[17]. Python eggs were briefly candled to locate embryos and major vessels, then windowed, and membranes and vessels were carefully detached from the inside of the shell to minimize damage. After FGF beads were implanted into a slit at the apex of python limb buds, the python eggs were resealed and incubated at 30 °C in a humidified box.

Received 27 January; accepted 24 March 1999.

1. Carroll, R. *Vertebrate Paleontology and Evolution* (Freeman, New York, 1988).
2. Lee, M. S. Y. & Caldwell, M. W. Anatomy and relationships of *Pachyrhachis problematicus*, a primitive snake with hindlimbs. *Phil. Trans. R. Soc. Lond. B* **353,** 1521–1552 (1998).
3. Gaunt, S. J. Conservation in the Hox code during morphological evolution. *Int. J. Dev. Biol.* **38,** 549–552 (1994).
4. Burke, A. C., Nelson, C. E., Morgan, B. A. & Tabin, C. Hox genes and the evolution of vertebrate axial morphology. *Development* **121,** 333–346 (1995).
5. Cohn, M. J. *et al. Hox9* genes and vertebrate limb specification. *Nature* **387,** 97–101 (1997).
6. Rancourt, D. E., Tsuzuki, T. & Capecchi, M. R. Genetic interaction between Hoxb-5 and Hoxb-6 is revealed by nonallelic noncomplementation. *Genes Dev.* **9,** 108–122 (1995).
7. Oliver, G., Wright, C. V., Hardwicke, J. & De Robertis, E. M. Differential antero-posterior expression of two proteins encoded by a homeobox gene in *Xenopus* and mouse embryos. *EMBO J.* **7,** 3199–3209 (1988).
8. Shashikant, C. S. *et al.* Regulation of *Hoxc-8* during mouse embryonic development: identification and characterization of critical elements involved in early neural tube expression. *Development* **121,** 4339–4347 (1995).
9. Wall, N. A., Jones, C. M., Hogan, B. L. & Wright, C. V. Expression and modification of Hox 2.1 protein in mouse embryos. *Mech. Dev.* **37,** 111–120 (1992).
10. Oliver, G., De Robertis, E. M., Wolpert, L. & Tickle, C. Expression of a homeobox gene in the chick wing bud following application of retinoic acid and grafts of polarizing region tissue. *EMBO J.* **9,** 3093–3099 (1990).
11. Nelson, C. E. *et al.* Analysis of Hox gene expression in the chick limb bud. *Development* **122,** 1449–1466 (1996).
12. Saunders, J. W. The proximo-distal sequence of origin of the parts of the chick wing and the role of the ectoderm. *J. Exp. Zool.* **108,** 363–402 (1948).
13. Fang, H. & Elinson, R. P. Patterns of distal-less gene expression and inductive interactions in the head of the direct developing frog *Eleutherodactylus coqui. Dev. Biol.* **179,** 160–172 (1996).
14. Ferrari, D. *et al.* The expression pattern of the Distal-less homeobox-containing gene Dlx-5 in the developing chick limb bud suggests its involvement in apical ectodermal ridge activity, pattern formation, and cartilage differentiation. *Mech. Dev.* **52,** 257–264 (1995).
15. Savage, M. P. *et al.* Distribution of FGF-2 suggests it has a role in chick limb bud growth. *Dev. Dyn.* **198,** 159–170 (1993).
16. Davidson, D. R., Crawley, A., Hill, R. E. & Tickle, C. Position-dependent expression of two related homeobox genes in developing vertebrate limbs. *Nature* **352,** 429–431 (1991).
17. Niswander, L., Jeffrey, S., Martin, G. R. & Tickle, C. A positive feedback loop coordinates growth and patterning in the vertebrate limb. *Nature* **371,** 609–612 (1994).
18. Laufer, E., Nelson, C. E., Johnson, R. L., Morgan, B. A. & Tabin, C. Sonic hedgehog and Fgf-4 act through a signaling cascade and feedback loop to integrate growth and patterning of the developing limb bud. *Cell* **79,** 993–1003 (1994).
19. Raynaud, A., Kan, P., Bouche, G. & Duprat, A. M. Fibroblast growth factors (FGF-2) and delayed involution of the posterior limbs of the slow-worm embryo (*Anguis fragilis*, L.). *C. R. Acad. Sci.* **318,** 573–578 (1995).
20. Altabef, M., Clarke, J. D. W. & Tickle, C. Dorso-ventral ectodermal compartments and origin of apical ectodermal ridge in developing chick limb. *Development* **124,** 4547–4546 (1997).
21. Zeller, R. & Duboule, D. Dorso-ventral limb polarity and origin of the ridge: on the fringe of independence? *BioEssays* **19,** 541–546 (1997).
22. Davis, C. A., Holmyard, D. P., Millen, K. J. & Joyner, A. L. Examining pattern formation in mouse, chicken and frog embryos with an En-specific antiserum. *Development* **111,** 287–298 (1991).
23. Riddle, R. D. *et al.* Induction of LIM homeobox gene *Lmx-1* by WNT7a establishes dorsoventral pattern in the vertebrate limb. *Cell* **83,** 631–640 (1995).
24. Chiang, C. *et al.* Cyclopia and defective axial patterning in mice lacking Sonic hedgehog gene function. *Nature* **383,** 407–413 (1996).
25. Marti, E., Takada, R., Bumcrot, D. A., Sasaki, H. & McMahon, A. P. Distribution of Sonic hedgehog peptides in the developing chick and mouse embryo. *Development* **121,** 2537–2547 (1995).
26. Marigo, V., Scott, M. P., Johnson, R. L., Goodrich, L. V. & Tabin, C. J. Conservation in hedgehog signaling: induction of a chicken patched homolog by Sonic hedgehog in the developing limb. *Development* **122,** 1225–1233 (1996).
27. Yang, Y. *et al.* Relationship between dose, distance and time in *Sonic Hedgehog*-mediated regulation of anteroposterior polarity in the chick limb. *Development* **124,** 4393–4404 (1997).
28. Charite, J., de Graaff, W., Shen, S. & Deschamps, J. Ectopic expression of Hoxb-8 causes duplication of the ZPA in the forelimb and homeotic transformation of axial structures. *Cell* **78,** 589–601 (1994).
29. Geduspan, J. S. & MacCabe, J. A. Transfer of dorsoventral information from mesoderm to ectoderm at the onset of limb development. *Anat. Rec.* **224,** 79–87 (1989).
30. Wilson, V. & Beddington, R. Expression of T protein in the primitive streak is necessary and sufficient for posterior mesoderm movement and somite differentiation. *Dev. Biol.* **192,** 45–58 (1997).
31. Panganiban, G., Sebring, A., Nagy, L. & Carroll, S. The development of crustacean limbs and the evolution of arthropods. *Science* **270,** 1363–1366 (1995).
32. Gasc, J.-P. Les rapports anatomiques du membre pelvien vestigial chez les squamates serpentiformes. *Bull. Mus. Nat. Hist. 2e Ser.* **38,** 99–110 (1966).
33. *Eyewitness Encyclopedia of Nature.* (Dorling-Kindersley Multimedia, London, 1995).

Acknowledgements. We thank Drayton Manor Zoo, Edinburgh Zoo, London Zoo, Welsh Mountain Zoo and J. Fletcher for fertile python eggs; M. Caldwell, A. Cohn, S. Evans, M. Ferguson, E. Kochva, M. Lee, C. O. Lovejoy, K. Patel, J. R. D. Stalvey, V. Wilson and L. Wolpert for discussion; M. Turmaine for assistance with scanning electron microscopy; and E. De Robertis, T. Jessell, A. Joyner, G. Martin, A. McMahon, G. Panganiban, C. Tabin, N. Wall, and R. Zeller for reagents. This research was funded by the BBSRC.

Correspondence and requests for materials should be addressed to M.J.C. (e-mail: M.J.Cohn@reading.ac.uk).

The MAPK kinase Pek1 acts as a phosphorylation-dependent molecular switch

Reiko Sugiura*, Takashi Toda†, Susheela Dhut†, Hisato Shuntoh‡ & Takayoshi Kuno*

** Department of Pharmacology, Kobe University School of Medicine, Kusunoki-cho, Chuo-ku, Kobe 650-0017, Japan*
† Cell Regulation Laboratory, Imperial Cancer Research Fund, PO Box 123, Lincoln's Inn Fields, London WC2A 3PX, UK
‡ Faculty of Health Science, Kobe University School of Medicine, 7-10-2 Tomogaoka, Suma-ku, Kobe 650-0142, Japan

The mitogen-activated protein kinase (MAPK) pathway is a highly conserved eukaryotic signalling cascade that converts extracellular signals into various outputs, such as cell growth and differentiation[1–3]. MAPK is phosphorylated and activated by a specific MAPK kinase (MAPKK)[4]: MAPKK is therefore considered to be an activating regulator of MAPK. Pmk1 is a MAPK that regulates cell integrity[5] and which, with calcineurin phosphatase, antagonizes chloride homeostasis[6] in fission yeast. We have now identified Pek1, a MAPKK for Pmk1 MAPK. We show here that Pek1, in its unphosphorylated form, acts as a potent negative regulator of Pmk1 MAPK signalling. Mkh1[7], an upstream MAPKK kinase (MAPKKK), converts Pek1 from being an inhibitor to an activator. Our results indicate that Pek1 has a dual stimulatory and inhibitory function which depends on its phosphorylation

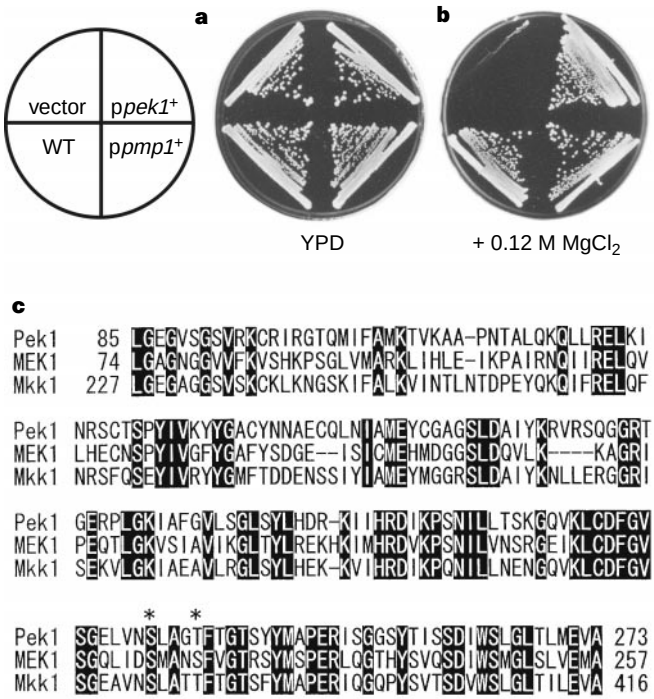

Figure 1 Isolation of Pek1. **a**, **b**, Suppression of the Cl^--sensitive growth defect of Δ*ppb1*. Δ*ppb1* cells that had been transformed with multicopy plasmid pDB248 (ref. 25) carrying either *ppb1*$^+$ (WT), *pek1*$^+$ (p*pek1*$^+$), *pmp1*$^+$ (p*pmp1*$^+$), or the vector alone, were streaked onto each plate, containing YPD medium (**a**) or YPD + 0.12 M $MgCl_2$ (**b**). Plates were incubated for 3 days at 33 °C. **c**, Amino-acid sequence alignment of Pek1, human MEK1 (GenBank accession number, L11284), and budding yeast Mkk1 (GenBank accession number, D13001). Filled boxes indicate conserved residues in all three proteins. Asterisks indicate potential phosphorylation sites (S234 and T238).